

Graph Neural Networks for Decentralized Multi-Robot Submodular Action Selection

Lifeng Zhou,^{1*} Vishnu D. Sharma,^{2*} Qingbiao Li,³ Amanda Prorok,³ Alejandro Ribeiro,¹ Vijay Kumar¹

Abstract—In this paper, we develop a learning-based approach for decentralized submodular maximization. We focus on applications where robots are required to jointly select actions, e.g., motion primitives, to maximize team submodular objectives with local communications only. Such applications are essential for large-scale multi-robot coordination such as multi-robot motion planning for area coverage, environment exploration, and target tracking. But the current decentralized submodular maximization algorithms either require assumptions on the inter-robot communication or lose some suboptimal guarantees. In this work, we propose a general-purpose learning architecture towards submodular maximization at scale, with decentralized communications. Particularly, our learning architecture leverages a graph neural network (GNN) to capture local interactions of the robots and learns decentralized decision-making for the robots. We train the learning model by imitating an expert solution and implement the resulting model for decentralized action selection involving local observations and communications only. We demonstrate the performance of our GNN-based learning approach in a scenario of active target coverage with large networks of robots. The simulation results show our approach nearly matches the coverage performance of the expert algorithm, and yet runs several orders faster with more than 30 robots. The results also exhibit our approach’s generalization capability in previously unseen scenarios, e.g., larger environments and larger networks of robots.

I. INTRODUCTION

Submodular maximization problems find a wealth of applications in robotics. Typical examples include environmental monitoring and surveillance [1], [2], target coverage and tracking [3], [4], [5], search and rescue [6], and informative path planning [7]. Such applications ask for teams of robots that act as mobile sensors to jointly plan their actions to optimize submodular objective functions. Submodular functions have the diminishing returns property. Examples of such functions include the information-theoretic metrics such as entropy and mutual information [1] and the geometric metrics such as the visibility region [8]. The problems of maximizing submodular functions are generally NP-hard. The most well-known approach for tackling these problems is the greedy algorithm that runs in polynomial time and yields a constant factor approximation guarantee [9], [10].

*These authors contributed equally.

¹L. Zhou, A. Ribeiro, and V. Kumar are with the GRASP Laboratory, University of Pennsylvania, Philadelphia, PA, USA (email: {lfzhou, aribeiro, kumar}@seas.upenn.edu).

²V. D. Sharma is with the Department of Computer Science, University of Maryland, College Park, MD, USA (email: vishnuds@umd.edu).

³Q. Li and A. Prorok are with the Department of Computer Science and Technology, University of Cambridge, Cambridge, United Kingdom (email: {q1295, asp45}@cam.ac.uk).

This research was sponsored by the Army Research Lab through ARL DCIST CRA W911NF-17-2-0181.

The greedy algorithm cannot be directly implemented in the scenarios where the robots can only communicate locally due to a limited communication range. To address the issue of local communication, some decentralized versions of the greedy algorithm were designed, where only neighboring information is utilized to choose actions for the robots for optimizing submodular objectives [11], [12], [13], [14]. However, these algorithms either assume a connected communication graph [11], [12] or typically have a worse suboptimality bound than that of the greedy algorithm [10] in the scenarios with limited communication [13], [14].

In this paper, we aim to explore learning-based methods that approach the performance of the greedy algorithm [10]. The graph neural network (GNN) is chosen as the learning method given its nice properties of decentralized communication architecture that captures the neighboring interactions and the transferability that allows for the generalization to previously unseen scenarios [15], [16]. Also, GNN has recently shown success in various multi-robot applications such as formation control [17], [18], path finding [19], and task assignment [20]. To this end, we design a GNN-based learning network that enables robots to communicate and share information with neighbors and selects actions for the robots. We train such a learning network to perform as close as possible to the greedy algorithm by imitating the behavior of the greedy algorithm.

Related Work. Researchers have developed several decentralized/distributed algorithms for tackling submodular maximization problems. For example, building on the local greedy algorithm [10, Section 4], Atanasov et al. designed a decentralized greedy algorithm that achieves 1/2 approximation bound for maximizing submodular objectives [11]. Specifically, the algorithm greedily selects an action for each robot in a sequential order, given all the actions selected so far. A speed-up of the sequential greedy algorithm was developed by Micah and Michael to select exploration actions for mobile robots [21]. However, with limited communication, the robots may not have access to all the previously selected actions. To this end, a few distributed submodular maximization algorithms were devised to execute the sequential greedy algorithm over directed acyclic graphs that may not be connected [13], [14]. The suboptimality bound of these distributed algorithms depends on the property of the communication graph and is typically worse than 1/2 [13], [14]. Particularly, the worst-case analysis parallels results in [22] where a distributed submodular maximization algorithm is developed for data selection. Other decentralized greedy approaches include the ones that utilize the consensus-based

mechanism [23] to bring robots to an agreement by communicating local greedy selections with neighbors over multiple hops [12], [24], [25]. However, these algorithms typically require the underlying communication graph is connected and may take a considerable amount of time to reach the consensus.

Recently, researchers have investigated learning-based methods, particularly GNN, to learn decentralized solutions that perform close to the centralized counterparts for multi-robot coordination [17], [18], [19], [20]. In particular, Tolstaya et al. implemented GNN to learn a decentralized flocking controller for a swarms of mobile robots by imitating a centralized flocking controller with global information. Similarly, Li et al. applied GNN to find collision-free paths for large networks of robots from start positions to goal positions in the obstacle-rich environments [19]. Their results demonstrated that, by mimicking a centralized expert solution, their decentralized path planner exhibits a near-expert performance, utilizing local observations and neighboring communication only, which also can be well generalized to larger teams of robots. They further improved the performance of their GNN-based approach [19] by introducing the attention mechanism [26] that intelligently adjusts communication strength based on relative importance of the information between robot and its neighbors [27]. The GNN-based approach was also investigated to learn solutions for the combinatorial optimization in a multi-robot task scheduling scenario [20]. These works inspire us to apply GNN-based approaches to tackle multi-robot coordination problems where the objectives are submodular functions.

Contributions. Overall, in this paper, we present a GNN-based learning approach for submodular maximization with local communications. Our approach goes beyond the decentralized greedy algorithms [11], [12], [13], [14] by allowing for disconnected communication graphs and aims for a near-centralized performance; and goes beyond the existing GNN-based learning methods [17], [18], [19], [20] by focusing on the multi-robot coordination with submodular objectives. Specifically, we make the following contributions:

- We formulate the problem of applying GNN for submodular action set selection for a team of robots with local communications (Problem 1);
- We design a GNN-based learning network that processes the robot’s individual observations and aggregates neighboring information to select an action set for the robots (i.e., the solution to Problem 1).
- We demonstrate the performance of our GNN-based learning approach such as the near-centralized behavior, transferability, and fast running time in the scenario of *active target coverage with large networks of robots*.

II. PRELIMINARIES

In this section, we introduce the basic notations and background knowledge which will be used throughout this paper. We begin by defining some notations as follows.

Calligraphic fonts denote sets (e.g., \mathcal{Y}). Given a set \mathcal{Y} , $2^{\mathcal{Y}}$ denotes its power set; $|\mathcal{Y}|$ denotes \mathcal{Y} ’s cardinality. Low-

ercase or uppercase letters, bold lowercase letters, and bold uppercase letters denote scalars (e.g., y or Y), vectors (e.g., \mathbf{y}) and matrices (e.g., \mathbf{Y}), respectively.

Next, we present the background on set functions and the greedy algorithm. We start with reviewing the useful properties of set functions such as monotonicity, submodularity, and matroid constraints. We then introduce the standard greedy algorithm for maximizing monotone submodular functions.

Normalized Function [9]: Given a finite ground set \mathcal{X} , a set function $f : 2^{\mathcal{X}} \mapsto \mathbb{R}$ is normalized if and only if one has $f(\emptyset) = 0$.

Monotonicity [9]: Given a finite ground set \mathcal{X} , a set function $f : 2^{\mathcal{X}} \mapsto \mathbb{R}$ is monotone (non-decreasing) if and only if for any sets $\mathcal{Y} \subseteq \mathcal{Y}' \subseteq \mathcal{X}$, one has $f(\mathcal{Y}) \leq f(\mathcal{Y}')$.

Submodularity [9, Proposition 2.1]: Given a finite ground set \mathcal{X} , a set function $f : 2^{\mathcal{X}} \mapsto \mathbb{R}$ is submodular if and only if for any sets $\mathcal{Y} \subseteq \mathcal{Y}' \subseteq \mathcal{X}$, and any element $x \in \mathcal{X}$, one has $f(\mathcal{Y} \cup \{x\}) - f(\mathcal{Y}) \geq f(\mathcal{Y}' \cup \{x\}) - f(\mathcal{Y}')$. In other words, the marginal gain of adding an element x , denoted by $f(\mathcal{Y} \cup \{x\}) - f(\mathcal{Y})$, is non-increasing, which captures the diminishing returns property of the submodular function.

Matroid [28, Section 39.1]: Given a finite set \mathcal{X} and a non-empty collection of subsets of \mathcal{X} , denoted by \mathcal{I} , the pair $(\mathcal{X}, \mathcal{I})$ is called a matroid if and only if one has the following conditions satisfied:

- for any set $\mathcal{Y} \subseteq \mathcal{X}$ such that $\mathcal{Y} \in \mathcal{I}$, and for any set $\mathcal{J} \subseteq \mathcal{Y}$, it must hold $\mathcal{J} \in \mathcal{I}$.
- for any sets $\mathcal{J}, \mathcal{Y} \subseteq \mathcal{X}$ and $|\mathcal{J}| \leq |\mathcal{Y}|$, it must hold that there exists an element $x \in \mathcal{Y} \setminus \mathcal{J}$ such that $\mathcal{J} \cup \{x\} \in \mathcal{I}$.

Particularly, a *partition matroid* is a matroid $(\mathcal{X}, \mathcal{I})$ such that for a positive integer n , positive integers $\kappa_1, \dots, \kappa_n$, and disjoint sets $\mathcal{X}_1, \dots, \mathcal{X}_n$ with $\mathcal{X} \equiv \mathcal{X}_1 \cup \dots \cup \mathcal{X}_n$, one has $\mathcal{I} = \{\mathcal{Y} : \mathcal{Y} \subseteq \mathcal{X}, |\mathcal{Y} \cap \mathcal{X}_i| \leq \kappa_i \text{ for all } i = 1, \dots, n\}$.

Greedy Algorithm [10] The greedy algorithm is an approximation algorithm that selects a set \mathcal{Y} from the ground set \mathcal{X} to optimize the function $f(\mathcal{Y})$. Specifically, it selects an element $x, x \in \mathcal{X}$ that renders the maximum marginal gain at each round, that is,

$$x^* = \operatorname{argmax}_{x \in \mathcal{X}} f(\mathcal{Y} \cup \{x\}) - f(\mathcal{Y}).$$

Clearly, the greedy algorithm runs in polynomial time. Also, for maximizing normalized monotone submodular set functions with a partition matroid, it gives a 1/2 approximation of the optimal [10]. That is,

$$\frac{f(\mathcal{Y}^g)}{f(\mathcal{Y}^*)} \geq \frac{1}{2}, \quad (1)$$

where $\mathcal{Y}^g \in \mathcal{I}$ is the set selected by the greedy algorithm with \mathcal{I} the partition matroid, and $\mathcal{Y}^* \in \mathcal{I}$ is the set selected by the optimal algorithm.

III. PROBLEM FORMULATION

We present the problem of *submodular maximization for decentralized multi-robot action selection*. Particularly, at each time step, the problem asks for selecting an action for

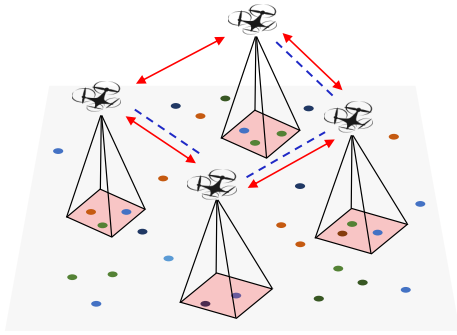


Fig. 1: Multi-robot target coverage: a team of aerial robots, mounted with down-facing cameras, aims at covering multiple targets (depicted as colorful dots) on the ground. The red arrow lines and the blue dotted lines show inter-robot observations and communications. The red squares represent the fields of views of the robots' cameras.

each robot to optimize a submodular team objective using local information only. For example, in a multi-robot active target coverage scenario (Fig. 1), the robots' actions are their candidate motion primitives, the team objective is the number of targets covered, and for each robot, the local information is the set of targets covered by it and its neighbors. The goal of this work is to implement GNN to learn such decentralized planning for the robots by *imitating* an expert algorithm. To this end, we start with introducing the framework of submodular action selection and GNN, and then formally define the problem.

A. Submodular Action Selection

a) *Robots*: We consider a team of N robots, denoted by $\mathcal{V} = \{1, 2, \dots, N\}$. At a given time step, the relative position between any two robots i and j in the environment is denoted by \mathbf{p}_{ij}^r , $i, j \in \mathcal{V}$. The global positions of the robots are not required.

b) *Action set*: We denote a set of *available actions* for each robot i as \mathcal{A}_i , $i \in \mathcal{V}$. At a given time step, the robot can select at most 1 action from its available action set, which follows the natural operational constraints: e.g., in a motion planning scenario, \mathcal{A}_i is robot i 's motion primitives, and the robot can select only 1 motion primitive to execute at each time step. For example, in Fig. 2, there are 2 robots, where robot 1's action set is $\mathcal{A}_1 = \{a_{1,1}, a_{1,2}, a_{1,3}\}$ (and robot 1 selects action $a_{1,1}$ to execute), and robot 2's action set is $\mathcal{A}_2 = \{a_{2,1}, a_{2,2}, a_{2,3}, a_{2,4}\}$ (and robot 2 chooses $a_{2,3}$ to execute). Denote the joint action set of all robots as $\mathcal{A} \triangleq \bigcup_{i \in \mathcal{V}} \mathcal{A}_i$. Also, denote a valid selection of actions for all robots as $\mathcal{U} \subseteq \mathcal{A}$. For example, we have $\mathcal{U} = \{a_{1,1}, a_{2,3}\}$ for the two robots in Fig. 2.

c) *Observation*: We consider each robot i is equipped with a sensor (e.g., a LiDAR sensor) to measure the relative positions to those robots that are within its sensing range (see Fig. 2). Without loss of generality, we assume all robots' sensors have the same *sensing range* r_s . For each robot i , we denote the set of robots within its sensing range as \mathcal{V}_i^s . Then the sensor observation of each robot i , i.e., the relative

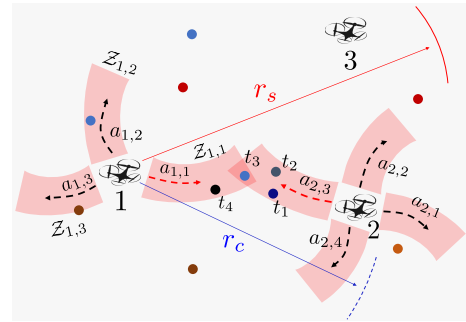


Fig. 2: Robots' observations, motion primitives, and communications: at a given time step, each robot observes those robots within its sensing range r_s ; e.g., robot 1 observes robot 2 and robot 3. Each robot has a set of motion primitives (depicted as dotted arrow curves), from which it can choose one to cover some targets using its camera. For example, robot 1 has 3 motion primitives, $\{a_{1,1}, a_{1,2}, a_{1,3}\}$, and it follows $a_{1,1}$ to cover 2 targets, $\{t_2, t_3\}$. Robot 2 has 4 motion primitives, $\{a_{2,1}, a_{2,2}, a_{2,3}, a_{2,4}\}$, and it chooses $a_{2,3}$ to cover 3 targets, $\{t_1, t_2, t_3\}$. However, in combination, these two motion primitives jointly cover 4 targets, $\{t_1, t_2, t_3, t_4\}$. In addition, each robot communicates with those robots within its communication range r_c ; e.g., robot 1 communicates with robot 2.

positions between robot i and \mathcal{V}_i^s , can be represented by $\mathcal{Z}_i^r = \{\mathbf{p}_{ij}^r\}_{j \in \mathcal{V}_i^s}$.

In addition, each robot is mounted with a camera that perceives a part of environment within its field of view (see Fig. 1). Using the camera, the robot can observe some objects and measure the relative positions to them in the environment, once it selects an action to execute. For example, in Fig. 2, when robot 1 selects motion primitive $a_{1,1}$, it can sweep and cover a set of targets $\{t_2, t_3\}$, and the corresponding observation $\mathcal{Z}_{1,1}$ is the relative positions to targets $\{t_2, t_3\}$. Notably, each action of the robot corresponds to an observation. Thus, given a time step, we denote the (possible) camera observation¹ of each robot i by \mathcal{Z}_i^t , which is the collection of the observations by the robot's available actions \mathcal{A}_i . For example, in Fig. 2, the camera observation of robot 1 is $\mathcal{Z}_1^t = \{\mathcal{Z}_{1,1}, \mathcal{Z}_{1,2}, \mathcal{Z}_{1,3}\}$. Particularly, we denote those objects that can be covered by robot i as \mathcal{T}_i and the corresponding relative positions as $\{\mathbf{p}_{ij}^t\}_{j \in \mathcal{T}_i}$. Then the robot i 's camera observation can be represented by $\mathcal{Z}_i^t = \{\mathbf{p}_{ij}^t\}_{j \in \mathcal{T}_i}$.

Finally, we define the observation of each robot i by \mathcal{Z}_i , which contains the observations of the sensor and camera on it, i.e., $\mathcal{Z}_i = \{\mathcal{Z}_i^r, \mathcal{Z}_i^t\}$.

d) *Communication*: Each robot $i \in \mathcal{V}$ communicates only with those robots within a prescribed *communication range*. Without loss of generality, we consider all robots have the same *communication range* r_c (see Fig. 2). That way, we introduce an (undirected) *communication graph* at a given time step as $\mathcal{G} = (\mathcal{V}, \mathcal{E}, \mathcal{W})$ with nodes the robots \mathcal{V} , edges $\mathcal{E} \subseteq \mathcal{V} \times \mathcal{V}$ the communication links, and weights of the edges $\mathcal{W} : \mathcal{E} \rightarrow \mathbb{R}$ denoting the strength of communications.

¹We call it as the possible observation, since the robot can select at most 1 action to execute at a time step.

The graph \mathcal{G} is distance-based and $(i, j) \in \mathcal{E}$ if and only if $\|\mathbf{p}_{ij}^e\|_2 \leq r_c$. We denote the *neighbors* of robot i by \mathcal{N}_i , which are the robots within the range r_c . \mathcal{N}_i is also called *1-hop neighbors* of robot i . We denote the adjacency matrix of graph \mathcal{G} by $\mathbf{S} \in \mathbb{R}^{N \times N}$ with $[\mathbf{S}]_{ij} = s_{ij} = 1$ if $(i, j) \in \mathcal{E}$ and 0 otherwise. Notably, the connectivity of graph \mathcal{G} is *not* required.

e) Objective function: We quantify the quality of the robots' actions \mathcal{U} by a monotone non-decreasing and sub-modular function $f : 2^{\mathcal{A}} \rightarrow \mathbb{R}$. For example, in the case of multi-robot active target coverage, f denotes the number of targets covered [3]. As shown in Fig. 2, the number of targets covered by the selected actions (motion primitives), $\mathcal{U} = \{a_{1,1}, a_{2,3}\}$, is $f(\mathcal{U}) = 4$.

B. Graph Neural Networks

a) Graph Shift Operation: We consider each robot $i, i \in \mathcal{V}$ has a feature vector $\mathbf{x}_i \in \mathbb{R}^F$, indicating the processed information of robot i . By collecting the feature vectors \mathbf{x}_i from all robots, we have the feature matrix for the robot team \mathcal{V} as:

$$\mathbf{X} = \begin{bmatrix} \mathbf{x}_1^T \\ \vdots \\ \mathbf{x}_N^T \end{bmatrix} = [\mathbf{x}^1, \dots, \mathbf{x}^F] \in \mathbb{R}^{N \times F}, \quad (2)$$

where $\mathbf{x}^f \in \mathbb{R}^N, f \in [1, \dots, F]$ is the collection of the feature f across all robots \mathcal{V} ; i.e., $\mathbf{x}^f = [\mathbf{x}_1^f, \dots, \mathbf{x}_N^f]^T$ with \mathbf{x}_i^f denoting the feature f of robot $i, i \in \mathcal{V}$. We conduct the *feature shift operation* for each robot i by a linear combination of its neighboring features, i.e., $\sum_{j \in \mathcal{N}_i} \mathbf{x}_j, j \in \mathcal{N}_i$. Hence, for all robots \mathcal{V} with graph \mathcal{G} , the feature matrix \mathbf{X} after the shift operation becomes $\mathbf{S}\mathbf{X}$ with:

$$[\mathbf{S}\mathbf{X}]_{if} = \sum_{j=1}^N [\mathbf{S}]_{ij} [\mathbf{X}]_j^f = \sum_{j \in \mathcal{N}_i} s_{ij} \mathbf{x}_j^f, \quad (3)$$

Here, the adjacency matrix \mathbf{S} is called the *Graph Shift Operator (GSO)* [16].

b) Graph convolution: With the shift operation, we define the *graph convolution* by a linear combination of the *shifted features* on graph \mathcal{G} via K -hop communication exchanges [16], [19]:

$$\mathcal{H}(\mathbf{X}; \mathbf{S}) = \sum_{k=0}^K \mathbf{S}^k \mathbf{X} \mathbf{H}_k, \quad (4)$$

where $\mathbf{H}_k \in \mathbb{R}^{F \times G}$ represents the coefficients combining F features of the robots in the shifted feature matrix $\mathbf{S}^k \mathbf{X}$, with F and G denoting the input and output dimensions of the graph convolution. Note that, $\mathbf{S}^k \mathbf{X} = \mathbf{S}(\mathbf{S}^{k-1} \mathbf{X})$ is computed by means of k communication exchanges with 1-hop neighbors.

c) Graph neural network: Applying a point-wise non-linearity $\sigma : \mathbb{R} \rightarrow \mathbb{R}$ as the activation function to the graph convolution (eq. (4)), we have the *graph perception* defined as:

$$\mathcal{H}(\mathbf{X}; \mathbf{S}) = \sigma \left(\sum_{k=0}^K \mathbf{S}^k \mathbf{X} \mathbf{H}_k \right). \quad (5)$$

Then, we define a GNN module by cascading L layers of graph perceptions (eq. (5)):

$$\mathbf{X}^\ell = \sigma[\mathcal{H}^\ell(\mathbf{X}^{\ell-1}; \mathbf{S})] \quad \text{for } \ell = 1, \dots, L, \quad (6)$$

where the output feature of the previous layer $\ell-1$, $\mathbf{X}^{\ell-1} \in \mathbb{R}^{N \times F^{\ell-1}}$, is taken as input to the current layer ℓ to generate the output feature of layer ℓ , \mathbf{X}^ℓ . Recall that the input to the first layer is $\mathbf{X}^0 = \mathbf{X}$ (eq. (2)). The output feature of the last layer $\mathbf{X}^L \in \mathbb{R}^{N \times G}$, obtained via K -hop communications and multi-layer perceptions, will be used to predict action set \mathcal{A} for all robots to the following problem.

C. Problem Definition

Problem (Decentralized submodular maximization for multi-robot action selection). *At each time step, the robots \mathcal{V} , by exchanging information with neighbors only over the communication graph \mathcal{G} , select an action to each robot $i \in \mathcal{V}$ to maximize a submodular objective function f :*

$$\begin{aligned} & \max_{\mathcal{U} \subseteq \mathcal{A}} f(\mathcal{U}) \\ & \text{s.t. } |\mathcal{U} \cap \mathcal{A}_i| = 1, \text{ for all } i \in \mathcal{V}. \end{aligned} \quad (7)$$

The constraint follows a partition matroid constraint to ensure that each robot selects 1 action per time step (e.g., 1 motion primitive among a set of motion primitives).

Eq. (7) can be interpreted as a submodular maximization problem with a partition matroid constraint and decentralized communication. This problem is generally NP-hard even if we assume the centralized communication [10]. That is because, finding the *optimal* action set requires to exhaustive search and evaluate the quality of *all possible* valid action sets $\mathcal{U} \subseteq \mathcal{A}$. Clearly, this exhaustive search method has combinatorial complexity and quickly becomes intractable as either the number of robots or the number of available actions of the robots increase. The most well-known approach for tackling this type of problem (with the centralized communication) is the (centralized) greedy algorithm [10] (see Section II). The advantage of the centralized greedy algorithm is two-fold: (i), it is efficient as it runs in polynomial time (with $O(|\mathcal{A}|^2)$ complexity); (ii), it achieves at least 1/2-approximation of the optimal (eq. (1)). In addition, since the 1/2-approximation bound is computed based on the worst-case performance, the centralized greedy algorithm can typically perform much better (on average) in practice; e.g., it performs close to the exhaustive search in small-scale cases (see Figure 4-a in Section V-D). Hence, in this paper, we use the centralized greedy algorithm as the *expert* algorithm to generate the ground-truth training data.

Particularly, we aim to train a learning network to perform as well as the centralized greedy algorithm for solving Eq. (7), while involving the communications among neighboring robots only. For such a learning network, GNN can be a great fit given its decentralized communication protocol. Hence, the goal is to utilize GNN to learn an action set \mathcal{U} to Eq. (7) by imitating the action set selected by the centralized greedy algorithm, denoted by \mathcal{U}^g . More formally, we define the problem of this work as follows.

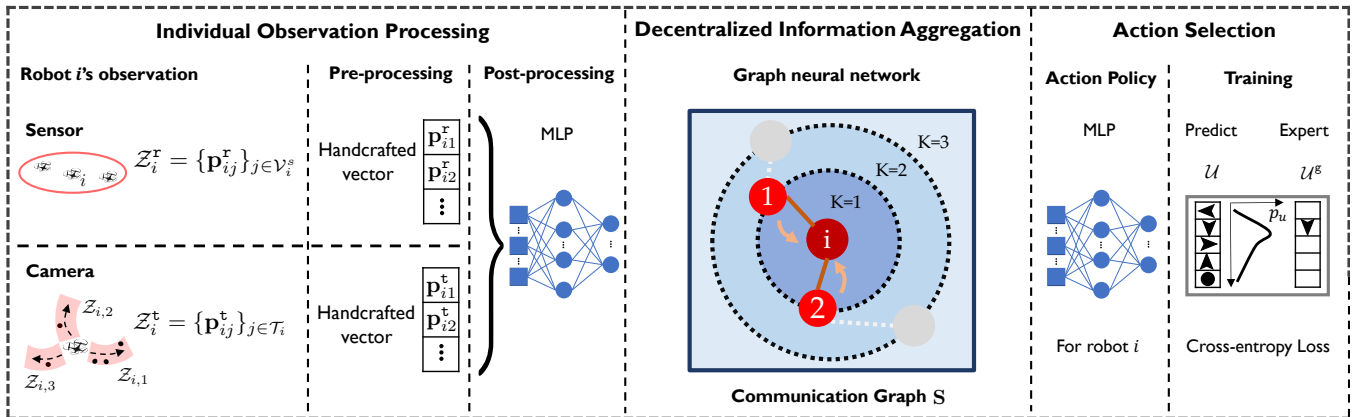


Fig. 3: Our decentralized learning architecture includes three main modules: (i), the Individual Observation Processing module processes the local observations and generates a feature vector for each robot; (ii), the Decentralized Information Aggregation module utilizes a GNN to aggregate and fuse the features from K -hop neighbors for each robot; (iii), the Decentralized Action Selection module selects an action for each robot by imitating an expert algorithm.

Problem 1. Design a GNN-based learning network to learn a mapping \mathcal{M} from the robots' observations $\{\mathcal{Z}_i\}_{i \in \mathcal{V}}$ and the communication graph \mathcal{G} to the robots' action set \mathcal{U} , i.e., $\mathcal{U} = \mathcal{M}(\{\mathcal{Z}_i\}_{i \in \mathcal{V}}, \mathcal{G})$, such that \mathcal{U} is as close as possible to \mathcal{U}^g .

We describe in detail our learning architecture for solving Problem 1 in the next section.

IV. ARCHITECTURE

We describe the key components of our learning architecture, illustrated in Fig. 3, as follows.

A. Individual Observation Processing

Recall that each robot i 's observation \mathcal{Z}_i includes its sensor observation \mathcal{Z}_i^r and its camera observation \mathcal{Z}_i^t (see Section III-A). We process the observation \mathcal{Z}_i to generate a feature vector \mathbf{x}_i for each robot i in two steps.

- Step 1 is a pre-processing step. Since the sensor observation \mathcal{Z}_i^r stores the relative robot positions $\{\mathbf{p}_{ij}^r\}_{j \in \mathcal{V}_i^s}$, we reshape (handcraft) it as a vector $\mathbf{x}_{i,1}^- := [\mathbf{p}_{i1}^r, \dots, \mathbf{p}_{i|\mathcal{V}_i^s|}^r]^\top$. Similarly, for the camera observation \mathcal{Z}_i^t that contains the relative positions to the objects covered, $\{\mathbf{p}_{ij}^t\}_{j \in \mathcal{T}_i}$, we reshape it as vector $\mathbf{x}_{i,2}^- := [\mathbf{p}_{i1}^t, \dots, \mathbf{p}_{i|\mathcal{T}_i|}^t]^\top$. Finally, by concatenating $\mathbf{x}_{i,1}^-$ and $\mathbf{x}_{i,2}^-$, we generate a pre-processed feature vector \mathbf{x}_i^- for robot i , i.e., $\mathbf{x}_i^- = [(\mathbf{x}_{i,1}^-)^\top, (\mathbf{x}_{i,2}^-)^\top]^\top$.
- Step 2 is a post-processing step where the pre-processed feature vector \mathbf{x}_i^- is fed into a multi-layer perceptron (MLP) module to generate the robot's feature vector \mathbf{x}_i , i.e., $\mathbf{x}_i = \text{MLP}(\mathbf{x}_i^-)$.

The feature vectors of the robots are then exchanged and fused through neighboring communications, described in Section IV-B.

B. Decentralized Information Aggregation

Each robot i communicates its feature (or processed information) with its neighbors \mathcal{N}_i over multiple communication

hops. As shown in Section III-B, for each robot i , we implement GNN to aggregate and fuse the feature vectors through K -hop communication exchanges among neighbors (eq. (4)). Thus, the output of the GNN (i.e., \mathbf{X}^L in eq. (6)) is a hyper-representation of the fused information of the robots and their K -hop neighbors. The output is then taken as input to the action selection module, described in Section IV-C, to generate an action for each robot. Notably, since only neighboring information is exchanged and fused, GNN renders a decentralized decision-making architecture.

C. Decentralized Action Selection

We aim at selecting an action set \mathcal{U} for the robots \mathcal{V} (1 action per robot) to maximize the team submodular objective function $f(\mathcal{U})$. To this end, we implement a MLP for each robot i to train an action selection module. More specifically, each robot applies a MLP that takes the aggregated features as input and selects an action for the robot as output. We consider all robots carry the same MLP, resembling a weight-sharing scheme. The action taken by each robot i is represented by a stochastic policy built on the probability distribution over its candidate actions $\mathcal{U}_i, i \in \mathcal{V}$. The actions of the robots are selected based on a supervised learning approach, described in Section IV-D.

D. Supervised Learning

Overall, our learning architecture consists of three main components—the Individual Observation Processing (Section IV-A), the Decentralized Information Aggregation (Section IV-B), and the Decentralized Action Selection module (Section IV-C). We train such a learning network by a supervised learning approach, i.e., to mimic an expert algorithm (the centralized greedy algorithm). Specifically, during the training stage, we have access to the action set \mathcal{U}^g selected by the centralized greedy algorithm, the corresponding observations on the robots $\{\mathcal{Z}_i\}_{i \in \mathcal{V}}$, and the corresponding communication graph \mathcal{G} . Thus, the training set \mathcal{D} can be constructed as a collection of these data,

i.e., $\mathcal{D} := \{(\{\mathcal{Z}_i\}_{i \in \mathcal{V}}, \mathcal{G}, \mathcal{U}^g)\}$. Over the training set \mathcal{D} , we train the mapping \mathcal{M} (defined in Problem 1) so that a cross entropy loss $\mathcal{L}(\cdot, \cdot)$, representing the difference between the output action set \mathcal{U} and the greedy action set \mathcal{U}^g is minimized. That is,

$$\min_{\text{PM}, \{\mathbf{H}_{\ell,k}\}, \text{MLP}} \sum_{(\{\mathcal{Z}_i\}_{i \in \mathcal{V}}, \mathcal{G}, \mathcal{U}^g) \in \mathcal{D}} \mathcal{L}(\mathcal{M}(\{\mathcal{Z}_i\}_{i \in \mathcal{V}}, \mathcal{G}), \mathcal{U}^g), \quad (8)$$

where we optimize over the learnable parameters of the processing method, named PM (e.g., CNN, MLP) to process the robots’ observations, the set of learnable parameter matrices $\{\mathbf{H}_{\ell,k}\}_{\ell \in \{1, \dots, L\}, k \in \{0, \dots, K\}}$ in GNN to aggregate and fuse the neighboring information over multiple communication hops, and the learnable parameters of MLP to select actions for the robots.

Notably, by the decentralized learning architecture where the parametrization is operated locally on each robot, the number of learnable parameters is independent of the number of the robots N . This decentralized parametrization offers a perfect complement to the supervised learning which requires the availability of expert solutions that can be costly in the large-scale settings. For example, even though the centralized greedy algorithm is much more efficient than the exhaustive search, it still takes considerable time to generate a solution when the number of robots or their actions is large, given its running time grows quadratically in the number of robots’ actions (i.e., with $O(|\mathcal{A}|^2)$ complexity). However, leveraging the decentralized parametrization, we only need to train over the small-scale cases and generalize the trained models such as the distributed computation (i.e., PM and MLP) and the neighboring information exchange (i.e., GNN) to the larger-scale settings, as it will be demonstrated in Section V-D. In other words, once trained, the learned models can be implemented in other cases, including those with different communication graphs and varying numbers of robots.

V. PERFORMANCE EVALUATION

We present the evaluations of our method in scenarios of *active target coverage with large networks of robots*. In particular, we compare our method with other baseline algorithms in terms of both running time and coverage quality. In these comparisons, we test the trained learning models in the cases with the same team size (the same number of robots) and the *previously unseen* team sizes (both smaller and larger number of robots). The code of implementations is available online.² The experiments are conducted using a 32-core, 2.10Ghz Xeon Silver-4208 CPU and an Nvidia GeForce RTX 2080Ti GPU with 156GB and 11GB of memory, respectively.

Next, we first describe the active target coverage scenario, the specifications of the learning architecture, and the compared baseline algorithms. Then we present the evaluations in detail.

²<https://github.com/VishnuDuttSharma/deep-multirobot-task>

A. Multi-Robot Multi-Target coverage

We consider N aerial robots that are tasked to track M ground targets. Each robot uses its sensor to obtain the relative positions to those robots that are within its sensing range r_s . The sensing range r_s is set to be $r_s = 20$ units.

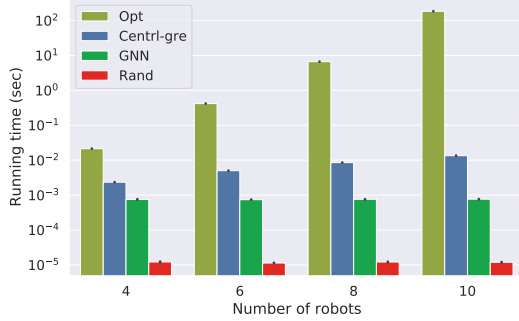
The camera on each robot i has a square field of view $d_o \times d_o$, and each robot i has 5 available motion primitives, $\mathcal{A}_i = \{\text{forward}, \text{backward}, \text{left}, \text{right}, \text{idle}\}$. Once the robot selects a motion primitive from $\mathcal{A}_i \setminus \text{idle}$, it flies a distance d_m along that motion primitive. If the robot selects the *idle* motion primitive, it stays still (i.e., $d_m = 0$). Hence, each motion primitive corresponds to a rectangular coverage region with length $d_m + d_o$ and width d_o . The coverage width (or the side of the field of view) is set to be $d_o = 6$ units. The flying length d_m is set to be $d_m = 8$ units for all robots selecting the non-*idle* motion primitive.

We set the robot’s communication range as $r_c = 20$ units and the communication hop as $K = 1$ (i.e., each robot i communicates only with its 1-hop neighbors \mathcal{N}_i). The objective function is considered to be the number of targets covered, given all robots selecting motion primitives.

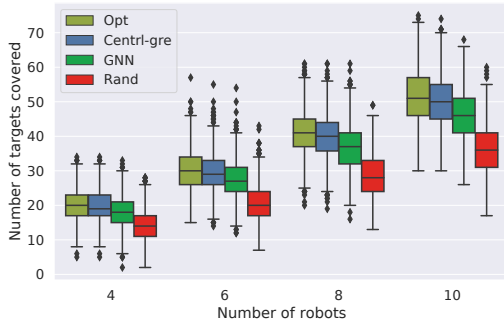
B. Supervised Learning Specification

We apply the centralized greedy algorithm [10] as the expert algorithm to generate a ground-truth data set. In each problem instance, we randomly generate the positions of the robots and targets in the environment, and utilize the centralized greedy algorithm to select an action set for the robots. Notably, each instance includes the robots’ observations $\{\mathcal{Z}_i\}_{i \in \mathcal{V}}$, the communication graph \mathcal{G} (represented by its adjacency matrix \mathbf{S}), and the greedy (or ground-truth) action set \mathcal{U}^g . The ground-truth data set comprises 120,000 instances for varying numbers of robots and the corresponding environments. In particular, we scale the size of the environment proportionally to the number of robots but keep the target density the same. Here, the target density is captured by the percentage of the cells in the grid occupied by the targets. We set the target density as 2.5% in all cases. The robot’s observations include the relative positions of 10 nearest robots within its sensing range and 20 nearest targets that can be covered. The data is randomly shuffled at training time and divided into a training set (60%), a validation set (20%), and a testing set (20%).

Our learning architecture consists of a 3-layer MLP with 32, 16, and 8 hidden layers as the Individual Observation Processing module, a 2-layer GNN with 32 and 128 hidden layers as the Decentralized Information Aggregation module, and a single layer MLP as the Decentralized Action Selection module. This learning network is implemented in PyTorch v1.6.0 and accelerated with CUDA v10.1 APIs. We use a learning rate scheduler with cosine annealing to decay the learning rate from 5×10^{-3} to 10^{-6} over 500 epochs with batch size 64. These learning modules and training parameters are selected from multiple experiments for parameter search.



(a) Running time (log scale).



(b) Number of targets covered.

Fig. 4: Small-scale comparison (averaged across 1000 trials) of Opt, Centrl-gre, GNN, and Rand in terms of running time and the number of targets covered.

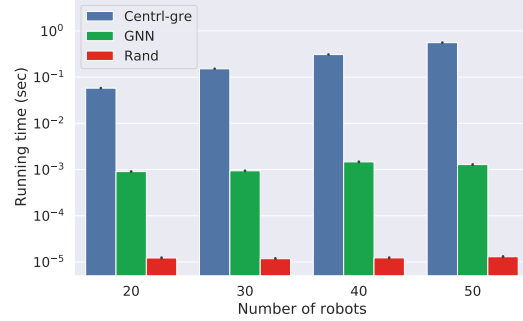
C. Compared Algorithms

We compare our method, named GNN with three other algorithms. The algorithms differ in how they select the robots' motion primitives. The first algorithm is the centralized greedy algorithm (the expert algorithm), named Centrl-gre. The second algorithm is an optimal algorithm, named Opt which attains the optimal solution for eq. (7) by exhaustive search. Particularly, for N robots, each with 5 motion primitives, Opt needs to evaluate 5^N possible cases to find the optimal solution. Evidently, Opt is viable only for small-scale cases. Hence, Opt is used for comparison only when the number of robots is small (e.g., $N \leq 10$). The third algorithm is a random algorithm, named Rand, which randomly (uniformly) selects one motion primitive for each robot.

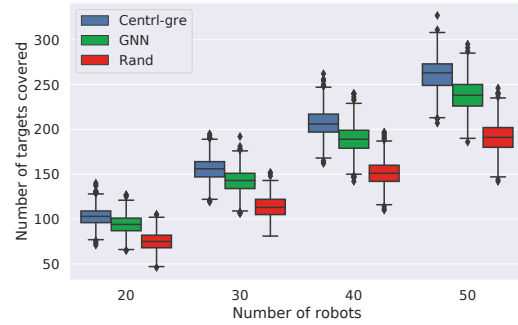
With the same settings, these four algorithms are compared in terms of the coverage quality, i.e., the number of targets covered, and the running time, across 1000 trials.

D. Evaluations

a) Small-scale comparison: We compare GNN with Centrl-gre, Opt and Rand in Figure 4. Since Opt is only feasible for small-scale scenarios, we set the number of robots $N = 4, 6, 8, 10$. Particularly, we train GNN with



(a) Running time (log scale).



(b) Number of targets covered.

Fig. 5: Large-scale comparison (averaged across 1000 trials) of Centrl-gre, GNN, and Rand in terms of running time and the number of targets covered.

the number of robots $N = 20$ and test its performance over $N = 4, 6, 8, 10$.

We observe GNN has a superior running time as shown in Figure 4-a: it runs considerably faster than both Centrl-gre and Opt: around 0.5 order faster than the former and 1.5 orders faster than the latter with 4 robots. This superiority becomes more significant as the number of robot increases. In addition, GNN has an average running time less than 1 ms, regardless of the number of robots, which is due to its decentralized decision-making protocol. Despite the considerably faster running time, GNN retains a coverage performance close to Centrl-gre and Opt and better than Rand: it covers in average more than 93% of the number of targets covered by Centrl-gre and more than 90% of that by Opt, and covers more targets than Rand with $N = 4, 6, 8, 10$, as shown in Figure 4-b.

Figure 4 also demonstrates the generalization capability of GNN in smaller-scale scenarios: even though it is trained with 20 robots, it maintains both fast running time and the coverage performance close to Centrl-gre and Opt with smaller number of robots, e.g., $N = 4, 6, 8, 10$. Another interesting observation is that Centrl-gre covers almost the same number of targets as Opt, and yet runs several orders faster when $N \geq 8$. This demonstrates the rationality of choosing Centrl-gre as the expert algorithm in this

Train \ Test	20	30	40	50
	20	46.66%	47.26%	47.08%
30	46.14%	46.81%	46.54%	46.53%
40	46.07%	46.79%	46.68%	46.79%

TABLE I: Percentage of the number of targets covered (the average across 1000 trials) by GNN trained and tested with varying numbers of robots.

target coverage scenario.

b) Large-scale comparison: We compare GNN with *Centrl-gre* and *Rand* in the large-scale scenarios where the number of robots is set as $N = 20, 30, 40, 50$. *Opt* is not included in this comparison due to long evaluation time. For only 10 robots, it takes almost two days to evaluate 1000 instances, each with 5^{10} possible cases. GNN is trained with the number of robots $N = 20$ and is tested over $N = 20, 30, 40, 50$. The results are reported in Figure 5. Similarly, we observe GNN runs around 1.5 to 2.5 orders faster than *Centrl-gre* with the running time around 1 ms for all $N = 20, 30, 40, 50$ (Figure 5-a). Although GNN runs faster, it achieves a coverage performance close to *Centrl-gre* and better than *Rand* (Figure 5-b). Additionally, these results verify GNN’s generalization capability in larger-scale scenarios: it is trained with 20 robots, and yet, can be well generalized to larger number of robots, e.g., $N = 30, 40, 50$.

c) Generalization evaluation: We further verify GNN’s generalization capability by evaluating the coverage quality of GNN trained and tested with varying numbers of robots. Specifically, we train GNN with $N = 20, 30, 40$ robots and test it on $N = 20, 30, 40, 50$ robots. The evaluation results are reported in Table I where the coverage quality is captured by the percentage of the number of targets covered with respect to the total number of the targets in the environment. We observe that GNN trained and tested with the *same* and *different* number of robots cover the similar percentage of the targets (around 46%), which further demonstrates the generalization capability of GNN.

To summarize, in the evaluations above, GNN provides a significant computational speed-up, and, yet, still attains a target coverage quality that nearly matches the quality of *Centrl-gre* and *Opt*. GNN also achieves a better coverage quality than *Rand*. In addition, GNN exhibits the capability of being able to well generalized to previously unseen scenarios.

VI. CONCLUSION AND FUTURE WORK

We worked towards choosing actions for the robots with local communications to maximize a submodular team objective function. Instead of designing classical decentralized submodular maximization algorithms (e.g., [11], [12], [13], [14]), we implemented a supervised learning approach that selects actions for the robots by imitating an expert solution. Particularly, we designed a GNN-based learning network that maps the robots’ individual observations and inter-robot

communications to the robots’ actions. We demonstrated the near-expert performance, generalization capability, and fast running time of the proposed approach.

This work opens up a number of future research avenues. One future direction is to incorporate the attention mechanism [19], [26] that weighs the relative importance of neighboring information into the current learning architecture. We expect the attention mechanism can prioritize the information of the neighbors with higher contributions. A second research avenue is to learn resilient coordination that secures team performance against either the malicious team members [29], [30] or adversarial outsiders [31], [32], [33].

REFERENCES

- [1] A. Krause, A. Singh, and C. Guestrin, “Near-optimal sensor placements in gaussian processes: Theory, efficient algorithms and empirical studies,” *Journal of Machine Learning Research*, vol. 9, no. Feb, pp. 235–284, 2008.
- [2] B. Grocholsky, J. Keller, V. Kumar, and G. Pappas, “Cooperative air and ground surveillance,” *IEEE Robotics & Automation Magazine*, vol. 13, no. 3, pp. 16–25, 2006.
- [3] P. Tokekar, V. Isler, and A. Franchi, “Multi-target visual tracking with aerial robots,” in *IEEE/RSJ International Conference on Intelligent Robots and Systems*, 2014, pp. 3067–3072.
- [4] P. Dames, P. Tokekar, and V. Kumar, “Detecting, localizing, and tracking an unknown number of moving targets using a team of mobile robots,” *The International Journal of Robotics Research*, vol. 36, no. 13-14, pp. 1540–1553, 2017.
- [5] L. Zhou and P. Tokekar, “Sensor assignment algorithms to improve observability while tracking targets,” *IEEE Transactions on Robotics*, vol. 35, no. 5, pp. 1206–1219, 2019.
- [6] V. Kumar and N. Michael, “Opportunities and challenges with autonomous micro aerial vehicles,” in *Robotics Research*. Springer, 2017, pp. 41–58.
- [7] A. Singh, A. Krause, C. Guestrin, and W. J. Kaiser, “Efficient informative sensing using multiple robots,” *Journal of Artificial Intelligence Research*, vol. 34, pp. 707–755, 2009.
- [8] H. Ding and D. Castanón, “Multi-agent discrete search with limited visibility,” in *Decision and Control (CDC), 2017 IEEE 56th Annual Conference on*. IEEE, 2017, pp. 108–113.
- [9] G. L. Nemhauser, L. A. Wolsey, and M. L. Fisher, “An analysis of approximations for maximizing submodular set functions—i,” *Mathematical programming*, vol. 14, no. 1, pp. 265–294, 1978.
- [10] M. L. Fisher, G. L. Nemhauser, and L. A. Wolsey, “An analysis of approximations for maximizing submodular set functions—ii,” in *Polyhedral combinatorics*. Springer, 1978, pp. 73–87.
- [11] N. Atanasov, J. Le Ny, K. Daniilidis, and G. J. Pappas, “Decentralized active information acquisition: Theory and application to multi-robot slam,” in *2015 IEEE International Conference on Robotics and Automation (ICRA)*. IEEE, 2015, pp. 4775–4782.
- [12] R. K. Williams, A. Gasparri, and G. Ulivi, “Decentralized matroid optimization for topology constraints in multi-robot allocation problems,” in *2017 IEEE International Conference on Robotics and Automation (ICRA)*. IEEE, 2017, pp. 293–300.
- [13] B. Ghahesifard and S. L. Smith, “Distributed submodular maximization with limited information,” *IEEE Transactions on Control of Network Systems*, vol. 5, no. 4, pp. 1635–1645, 2018.
- [14] D. Grimsman, M. S. Ali, J. P. Hespanha, and J. R. Marden, “The impact of information in greedy submodular maximization,” *IEEE Transactions on Control of Network Systems*, 2018.
- [15] L. Ruiz, F. Gama, and A. Ribeiro, “Graph neural networks: Architectures, stability, and transferability,” *Proceedings of the IEEE*, 2021.
- [16] F. Gama, A. G. Marques, G. Leus, and A. Ribeiro, “Convolutional neural network architectures for signals supported on graphs,” *IEEE Transactions on Signal Processing*, vol. 67, no. 4, pp. 1034–1049, 2019.
- [17] E. Tolstaya, F. Gama, J. Paulos, G. Pappas, V. Kumar, and A. Ribeiro, “Learning decentralized controllers for robot swarms with graph neural networks,” in *Conference Robot Learning 2019*. Osaka, Japan: Int. Found. Robotics Res., 30 Oct.-1 Nov. 2019.

- [18] A. Khan, E. Tolstaya, A. Ribeiro, and V. Kumar, "Graph policy gradients for large scale robot control," in *Conference on Robot Learning*, 2020, pp. 823–834.
- [19] Q. Li, F. Gama, A. Ribeiro, and A. Prorok, "Graph neural networks for decentralized multi-robot path planning," in *2020 IEEE/RSJ International Conference on Intelligent Robots and Systems (IROS)*. IEEE, 2020.
- [20] Z. Wang and M. Gombolay, "Learning scheduling policies for multi-robot coordination with graph attention networks," *IEEE Robotics and Automation Letters*, vol. 5, no. 3, pp. 4509–4516, 2020.
- [21] M. Corah and N. Michael, "Distributed matroid-constrained submodular maximization for multi-robot exploration: Theory and practice," *Autonomous Robots*, vol. 43, no. 2, pp. 485–501, 2019.
- [22] B. Mirzasoleiman, A. Karbasi, R. Sarkar, and A. Krause, "Distributed submodular maximization: Identifying representative elements in massive data," in *Advances in Neural Information Processing Systems*, 2013, pp. 2049–2057.
- [23] R. Olfati-Saber and R. M. Murray, "Consensus problems in networks of agents with switching topology and time-delays," *IEEE Transactions on automatic control*, vol. 49, no. 9, pp. 1520–1533, 2004.
- [24] G. Qu, D. Brown, and N. Li, "Distributed greedy algorithm for multi-agent task assignment problem with submodular utility functions," *Automatica*, vol. 105, pp. 206–215, 2019.
- [25] J. Liu and R. K. Williams, "Submodular optimization for coupled task allocation and intermittent deployment problems," *IEEE Robotics and Automation Letters*, vol. 4, no. 4, pp. 3169–3176, 2019.
- [26] A. Vaswani, N. Shazeer, N. Parmar, J. Uszkoreit, L. Jones, A. N. Gomez, L. Kaiser, and I. Polosukhin, "Attention is all you need," *arXiv preprint arXiv:1706.03762*, 2017.
- [27] Q. Li, W. Lin, Z. Liu, and A. Prorok, "Message-aware graph attention networks for large-scale multi-robot path planning," *IEEE Robotics and Automation Letters*, 2021.
- [28] A. Schrijver, *Combinatorial optimization: polyhedra and efficiency*. Springer Science & Business Media, 2003, vol. 24.
- [29] J. Blumenkamp and A. Prorok, "The emergence of adversarial communication in multi-agent reinforcement learning," *arXiv preprint arXiv:2008.02616*, 2020.
- [30] K. Saulnier, D. Saldana, A. Prorok, G. J. Pappas, and V. Kumar, "Resilient flocking for mobile robot teams," *IEEE Robotics and Automation letters*, vol. 2, no. 2, pp. 1039–1046, 2017.
- [31] L. Zhou, V. Tzoumas, G. J. Pappas, and P. Tokekar, "Resilient active target tracking with multiple robots," *IEEE Robotics and Automation Letters*, vol. 4, no. 1, pp. 129–136, 2018.
- [32] —, "Distributed attack-robust submodular maximization for multi-robot planning," in *2020 IEEE International Conference on Robotics and Automation (ICRA)*. IEEE, 2020, pp. 2479–2485.
- [33] G. Shi, L. Zhou, and P. Tokekar, "Robust multiple-path orienteering problem: Securing against adversarial attacks," in *2020 Robotics: Science and Systems (RSS)*, 2020.